HMG Advance Access published May 20, 2007



# Mutations in splicing factor PRPF3, causing retinal degeneration, form detrimental aggregates in photoreceptor cells

Antonella Comitato[1§], Carmine Spampanato[2§], Christina Chakarova[3], Daniela Sanges[1,2], Shomi S. Bhattacharya[3], Valeria Marigo[1,*]

[1] Department of Biomedical Sciences, University of Modena and Reggio Emilia, Modena, Italy

[2] Telethon Institute of Genetics and Medicine (TIGEM), Naples, Italy

[3] Department of Molecular Genetics, Institute of Ophthalmology, UCL, London, UK

[§] The authors wish it to be known that, in their opinion, the first two authors should be regarded as joint First Authors

* corresponding author: Department of Biomedical Sciences, University of Modena and Reggio Emilia, via Campi 287, 41100 Modena, Italy; telephone: +390592055392, fax: +390592055410, e-mail: marigo.valeria@unimore.it

**Abstract**

PRPF3 is an element of the splicing machinery ubiquitously expressed, yet mutations in this gene are associated with a tissue specific phenotype: autosomal dominant retinitis pigmentosa (RP). Here we studied the subcellular localization of endogenous and mutant transfected PRPF3. We found that: (i) subcellular distribution of the endogenous wild type protein co-localizes with snRNPs, partially with a nucleolar marker and accumulates in speckles labeled by SC35; (ii) in human retinas *PRPF3* does not show a distinctive abundance in photoreceptors, the cells affected in RP; (iii) RP causing mutant PRPF3, differently from the wild type protein, forms abnormally big aggregates in transfected photoreceptor cells. Aggregation of T494M mutant PRPF3 inside the nucleus triggers apoptosis only in photoreceptor cells. Based on the observation that mutant PRPF3 accumulates in the nucleolus and that transcriptional, translational and proteasome inhibition can induce this phenomenon in non-photoreceptor cells, we hypothesize that mutation affects splicing factor recycling. Noteworthy, accumulation of the mutant protein in big aggregates also affects distribution of some other splicing factors. Our data suggest that the mutant protein has a cell specific dominant effect in rod photoreceptors while appears not to be harmful to epithelial and fibroblast cells.

## INTRODUCTION

Retinitis Pigmentosa (RP) is a genetically heterogeneous disease and can be inherited as autosomal dominant, autosomal recessive and X-linked trait. Many genes mutated in RP have a tissue specific expression in the eye and are either components of the phototransduction cascade or of the visual cycle or structural proteins of photoreceptor cells. In contrast, in the last years, four pre-mRNA splicing factors have been linked to autosomal dominant RP. *PRPF31* was found mutated in RP11 patients (1), RP13 is due to mutations in the *PRPF8* gene (2), PAP-1 underlies RP9 (3) and mutations in the *PRPF3* gene cause RP18 (4). RP18 patients show a typical RP phenotype starting at the end of the first decade of life (5). Two different missense mutations in English, Danish and Spanish families have been identified in the *PRPF3* gene and they are localized in two adjacent amino acids of the C-terminal portion of the protein, a region well conserved in evolution (4, 6). The link between mutant PRPF3 and retinal degeneration is completely obscure. It is unclear why mutations in a ubiquitously expressed gene cause such a specific phenotype.

The yeast homologs of PRPF3, PRPF31 and PRPF8 are part of the U4/U6+U5 spliceosome trimer. Splicing of pre-mRNA is catalyzed in the nucleus by a large ribonucleoprotein complex, the spliceosome. The spliceosome consists of the pre-mRNA substrate and several small nuclear ribonucleoproteins (snRNPs) together with non-RNP splicing factors. Each snRNP particle consists of one (U1, U2 and U5) or two (U4/U6) snRNAs associated with many auxiliary proteins. The U6 snRNP is chemically modified by snoRNA in the nucleolus before its final assembly into the U6 snRNP. PRPF31 is part of U4/U6+U5 trimer (7) while PRPF8 contacts both the 5’ and 3’ splice sites of the intron as well as U6 RNA (8). Interaction of PRPF3 protein with PRP4, a key component of the U4/U6 splicing complex, defined PRPF3 as an snRNP (9). Deletion analysis of the PRPF3 protein showed that the central region (amino acids 195-442) binds PRP4 in the U4/U6 complex

while the C-terminal part of the protein is involved in binding with snRNAs (9) and with PAP-1 (10). Not all splicing factors are always bound to pre-mRNA and assembled into active spliceosomes *in vivo*. Therefore labeling of a splicing factor will detect not only sites of splicing but also sites of assembly, transport or storage. snRNPs and non-snRNP splicing factors localize in the nucleus in a characteristic speckled pattern. The pattern typically contains 20-40 intensely stained speckles against a diffuse nuclear population of splicing factors. While PRPF3 is biochemically defined as snRNP, its expression pattern, subnuclear localization in mammalian cells and association with different nuclear structures have not been characterized in detail yet.

The aim of our study was to define the molecular mechanism underlying photoreceptor cell death caused by PRPF3 mutations. We show that mutations found in RP patients cause mislocalization of the PRPF3 protein in a photoreceptor cell line. Aggregation in the nucleolus of mutant PRPF3 affects nuclear distribution of other splicing factors. Aberrant behavior of mutant PRPF3 is followed by activation of programmed cell death. This phenomenon cannot be observed in epithelial or fibroblast cell lines. We otherwise found that a similar phenotype can be caused in non-photoreceptor cells when either transcription or translation or proteasome are inhibited. Our data provide evidence that disease causing mutations are associated with aberrant protein aggregation in photoreceptors and that this may be related to defects in recycling of the pre-mRNA splicing factor.

## RESULTS

### *PRPF3* localization in the retina

Previous studies based on RT-PCR showed ubiquitous expression of human *PRPF3* (4) but this analysis did not allow a resolution of transcript distribution at a cellular level. We therefore analyzed PRPF3 protein localization in sections of adult human retina. PRPF3

protein was localized to the nuclei of photoreceptor cells, interneurons and ganglion cells. Relatively higher levels were detected in ganglion and inner nuclear layers and lower levels in the outer nuclear layer where photoreceptors are localized (Figure 1A). Similarly, murine *Prpf*3 mRNA showed an uneven distribution in the adult where a prevalent expression was detected in ganglion cells and in the inner nuclear layer (Supplementary figure 1B). Higher levels of expression were detected 8 days after birth (P8) in the outer nuclear layer of a not fully developed retina when rods have not completed their differentiation yet (Supplementary figure 1A).

**Subcellular distribution of wild type and mutant PRPF3**

In order to characterize subcellular distribution of endogenous PRPF3 we compared PRPF3 protein localization with known proteins labeling different nuclear compartments in HeLa cells. PRPF3 co-localized with snRNPs inside the nuclei (Figure 1B-D) and also partially overlapped with splicing nuclear speckles detected with an antibody to the SC35 protein, a non-snRNP splicing factor of the SR family of proteins (Figure 1E-G). Low amount of PRPF3 was observed inside the nucleolus, as shown by co-localization with the nucleolar marker fibrillarin (Figure 1 H-J, arrow). PRPF3 staining inside the nucleolus varied from cell to cell when compared to fibrillarin suggesting that PRPF3, as other snRNPs, transiently enter the nucleolus. Conversely, we detected no co-localization of PRPF3 with coilin, that labels Cajal bodies (Figure 1K-M).

In order to define whether mutations found in RP patients affected localization of PRPF3, we cloned human PRPF3 in frame with EGFP at the N-terminus. The use of tagged wild type, P493S mutant and T494M mutant PRPF3 was motivated by the requirement to distinguish transfected proteins from the endogenous protein. Transfected wild type PRPF3 localized to the nucleus of HeLa cells with a dot-like pattern, and more abundantly in the

nucleolus when compared to endogenous PRPF3 (Figure 1N, arrow). Similarly to the wild type protein, both mutations found in patients were observed inside the nucleus of transfected cells, in dot-like structures and in the nucleolus (Figure 1O and P). To rule out the possibility that subcellular localization of the transfected proteins was affected by the EGFP tag, we cloned wild type and mutant PRPF3 in frame with a His tag at the C-terminus and obtained identical results (data not shown). Therefore transfected protein localized in speckles (as seen by co-localization with SC35, figure 5) however over-expression causes storage of extra protein in the nucleolus.

**Aberrant and detrimental behavior of mutant PRPF3 in a photoreceptor cell line**

Wild type and mutant PRPF3 showed a similar subcellular localization in epithelial cells in culture. However, mutations in patients cause a specific phenotype in rod photoreceptors. We therefore tested subcellular distribution in *in vitro* cultured photoreceptor cells. 661W cells are a good model for *in vitro* studies of photoreceptors because they are an immortalized mouse cell line derived from transgenic mice expressing the SV40 T antigen under the control of the photoreceptor specific IRBP promoter (11). These cells, under regular culture conditions, do not show a very specific morphological and molecular photoreceptor phenotype (Supplementary figure 1C). Treatment of 661W cells with sodium butyrate, as previously reported for Y79 human photoreceptor tumor cells (12), induced differentiation as shown by elongated shape, upregulation of rhodopsin and phosphodiesterase 6β (Supplementary figure 1D) and reduction of progenitor marker nestin (Supplementary figure 1G-H). Differently from Y79, treatment of 661W with sodium butyrate did not activate apoptosis (Figure 4B and D). We also observed that sodium butyrate reduced expression of endogenous Prpf3 (Supplementary figure 1E-F). This result was in line with the observation that *in vivo* expression in photoreceptors decreased upon differentiation (Supplementary

figure 1A-B). These findings, together with the previous characterization of this cell line (11), confirmed that 661W in the presence of sodium butyrate can be a valuable system for functional studies in photoreceptor cells. Hence, we transfected wild type and mutant EGFP tagged PRPF3 in 661W cells and we allowed *in vitro* differentiation by treatment with sodium butyrate. Wild type PRPF3 localized to the nucleus of photoreceptors with a dot-like pattern in addition to a diffuse staining (Figure 2A-B). On the contrary, T494M mutant PRPF3 accumulated in a big aggregate inside the nucleus (Figure 2D, arrow). Formation of big aggregates was subsequent to treatment with sodium butyrate of 661W cells (Figure 2C-D). By introducing a negatively charged residue (aspartate, T494D), that may mimic the effect of putative phosphorylation at the threonine residue (13), we generated a different mutation in amino acid 494 of PRPF3 protein. Interestingly, T494D mutant behaves like the wild type protein (Figure 2E). Similar results were obtained with P493S mutant protein and with differently tagged constructs (Supplementary Figure 2).

In order to define whether mutant PRPF3 behaved abnormally also in photoreceptors *in vivo*, we electroporated neonatal murine eyes with the EGFP tagged constructs and analyzed protein distribution 13 days later, when photoreceptor cells differentiated. While wild type PRPF3 localized with a dot-like pattern inside the nuclei of electroporated photoreceptors (Figure 3A), T494M mutant PRPF3 formed, similarly to 661W cells *in vitro*, a big aggregate detectable inside photoreceptor nuclei (Figure 3B).

We speculated that aggregation of a pre-mRNA splicing factor could affect distribution of other components of the splicing machinery and found SC35 in the aggregate together with the mutant PRPF3 (Figure 2F-K). Differently, no major change of other snRNPs was induced by expression of mutant PRPF3 (Figure 2L-Q).

Finally, we assessed whether aggregation of mutant PRPF3 is detrimental to photoreceptors *in vitro*. No TUNEL positive cells were detected after transfection of the wild

type protein with or without sodium butyrate (Figure 4A-D and I), on the contrary expression of T494M mutant PRPF3 in the presence of sodium butyrate strictly correlated with chromatin fragmentation and apoptosis (Figure 4E-H). A time course experiment showed that 12 hours after transfection aggregation of T494M mutant PRPF3 could be observed in 25% of transfected cells however no apoptosis could be detected by TUNEL staining yet. Six hours later the number of T494M PRPF3 expressing cells decreased compared to wild type transfected cells suggesting that cell demise occurred. Consistently, most of the transfected cells showed amassed nuclear T494M PRPF3 and chromatin fragmentation and 36 hours after transfection no cell that expressed mutant PRPF3 could be found (Figure 4I). Similar experiments were performed in HeLa and NIH3T3 cells (Supplementary figure 3G-L and data not shown) and, unlike as presented with 661W cell line, no indication of apoptosis was observed.

**Nuclear distribution of mutant PRPF3 is affected by transcription, translation and proteasome inhibition**

Aggregation of mutant PRPF3 appears to be cell type specific and this may be correlated to specific physiological conditions of differentiated photoreceptors. Previous studies showed that treatment of cells with transcriptional inhibitors reduces splicing activity and foci associated with RNA processing undergo dynamic changes, in particular, speckles labeled with SC35 become fewer, increase in size and round up (14). To determine whether localizations of wild type and mutant PRPF3 could be affected by the transcriptional activity of the cell, transfected HeLa cells were treated with actinomycin D, inhibitor of nucleolar RNA and mRNA synthesis, or α-amanitin, inhibitor of transcription mediated by RNA polymerase II. Similar results were observed with both drugs, but a stronger phenotype was observed when both mRNA and nucleolar RNA syntheses were inhibited. Inhibition of

transcription caused wild type PRPF3 to diffuse inside the nucleus and to lose the dot-like pattern (Figure 5A), on the contrary T494M mutant PRPF3 accumulated in a single big mass (Figure 5D). We also observed that the abnormal behavior of mutant PRPF3 caused changes in the distribution of SC35 (Figure 5E-F), preventing it to form typical big speckles (Figure 5B). Similarly, inhibition of either protein synthesis or proteasome caused abnormal behavior of T494M mutant PRPF3 that formed big masses aggregating with SC35 (Figure 5G-R). When we analyzed localization of other snRNPs we found that after treatment with proteasome inhibitor, Y12 completely co-localized with wild type PRPF3 and only partially co-localized with mutant PRPF3 in the big aggregate (Figure 5S and T).

Formation of aggregates inside the nucleus was specific for these treatments. In fact, treatment with sodium butyrate, a histone deacetylase inhibitor, or thapsigargin, that inhibits ER-associated $Ca^{2+}$-ATPase and disrupts $Ca^{2+}$ homeostasis, did not cause changes in subcellular distribution of mutant PRPF3 that behaved like the wild type protein (Supplementary figure 3).

We finally wanted to characterize in which nuclear compartment T494M mutant PRPF3 aggregated. We performed double labeling of transfected cells with other markers of different nuclear compartments. Mutant PRPF3 formed a single big aggregate co-localizing with nucleolar marker fibrillarin (Figure 5U).

## DISCUSSION

In the recent years four genes encoding pre-mRNA splicing factors have been associated to autosomal dominant RP. They are all component of the U4/U6.U5 tri-snRNP complex, and this suggests that mutations in these genes may activate a common detrimental pathway in photoreceptor cells. The mechanism by which mutations in pre-mRNA splicing factor proteins cause the selective demise of photoreceptors is currently unknown. In fact, a direct

link between the function of U4/U6.U5 tri-snRNP complex and photoreceptor cells has not been discovered and expression analyses of these genes did not support a cell specific function (2-4, 15).

In this study we report tissue and subcellular distribution of endogenous PRPF3. Protein localization experiments did not show prevalent *PRPF3* expression in photoreceptors, the cells that undergo degeneration in RP patients. Subcellular distribution is consistent with previous studies characterizing PRPF3 as a pre-mRNA splicing factor (16, 17). Nuclear localization was similar to other snRNPs, and also partially concentrated in speckles as shown by co-localization with the SR protein SC35. Interestingly, we observed low amounts of the protein inside the nucleolus. Some of the U4/U6.U5 tri-snRNP complex components, like U6 snRNP, are modified in the nucleolus before final assembly. Similarly, PRPF3 may require chemical modifications in the nucleolus to become active.

Our analysis of wild type versus mutant PRPF3 brought to light an abnormal behavior of the protein subsequent to mutations found in RP patients. Interestingly, this phenotype manifested only upon differentiation to photoreceptors. This indicates that the abnormal behavior requires either a cell specific factor expressed in differentiated rods or a metabolic change consequent to differentiation. This last hypothesis is supported by previous reports describing reorganization of subnuclear structures during neuronal differentiation (18). Of note is the observation that aggregation of mutant PRPF3 can also be caused by changes in transcriptional activities or protein translation and degradation. As spliceosome assembly is a dynamic and reversible process, it is possible that mutant PRPF3 is sensitive to the turnover determined by proteasome-mediated degradation. In fact proteasome inhibition may stabilize the dynamic interaction of mutant PRPF3 with other splicing factors in the nucleolar region. A similar effect was previously reported on interaction of Myc and PML in the nucleolus (19). Our data indicate a defect in recycling of mutant PRPF3 in these stressful conditions. It

is known that in the absence of nascent RNAs, as in conditions of transcriptional inhibition, splicing factors cannot find a target and therefore they return to their storage or assembly sites (14, 20). This can be visualized by rounding up of speckles containing SC35 in response to transcription inhibitors and diffuse staining of snRNP proteins. On the contrary, mutant PRPF3 amassed in big aggregates in the nucleolus and this affects also localization of SC35. Other snRNPs (sm proteins) are otherwise only marginally affected by mutant PRPF3. This can be due to specific properties of distinct splicing factors that can reside in different nuclear compartments for shorter or longer time and specifically in the nucleolus. We also observed that mutant PRPF3, from a condition similar to the wild type protein, slowly accumulated in a big protein mass close to the nucleolar region. Interestingly, this behavior is similar to the Smn protein, mutated in spinal muscular atrophy, that was shown to co-localize with fibrillarin in the nucleolus of neurons, and this raised the hypothesis of a neuronal specific function of this protein (21). The formation of aggregates appears to be specific to the mutation Threonine 494 to Methionine, because mutation of the threonine to an acidic amino acid behaves like the wild type protein. Noteworthy, the specific mutation T494M has been found several times in RP18 patients and no founder effect was demonstrated (4, 6).

In conclusion, our data suggest that mutant PRPF3 causes mislocalization of splicing factors and forms aggregates that can be detrimental to the photoreceptor cell. We can envision the possibility that the pathogenetic mechanism is similar also for mutations in other pre-mRNA splicing factors. In fact, downregulation of PRPF31 inhibits formation of U4/U6.U5 tri-snRNP causing accumulation of snRNPs in bigger nuclear speckles (22). Further studies are needed to define whether aggregates found with mutant PRPF3 and those caused by haploinsufficiency of PRPF31 have similar effects on other splicing factors in the nucleus and whether they impair splicing of rod specific genes. Two possible outcomes can develop from PRPF3 mutation: the mutation leads to haploinsufficiency or the mutant protein has a

cell specific dominant negative effect in photoreceptor cells only. With all the above evidence shown in this paper we favor the second hypothesis. In fact we demonstrated a detrimental behavior of mutant PRPF3 only upon differentiation of rod photoreceptor cells. Future studies will address biochemical changes underlying the formation of nuclear aggregates by mutant PRPF3.

## MATERIALS AND METHODS

### *PRPF3* constructs

Human wild type and mutant (P493S and T494M) *PRPF3* were cloned in the pTriEx-1 expression vector (Novagen, La Jolla, CA, USA) using *EcoRV* and *XhoI* restriction sites.

EGFP-PRPF3- pTriEx-1, wild type and T494M mutant, were generated by amplification with Pfu DNA polymerase (Promega, Milan, Italy) starting from PRPF3 in pTriEx-1 (wild type and T494M) using as primers: 5'HPRPF3: CGGAATTCGCACTGTCAAAGAGGGAGCTG and 3'HPRP3: CGGGATCCAATCACTTAGTGATGGTGATG. The PCR products were cloned in the pTriEx-1 expression vector in which EGFP was cloned at the *XbaI-XhoI* sites to obtain a PRPF3 tagged at the N-terminal (Novagen. La Jolla, CA, USA).

T494D mutant *PRPF3* was generated by DNA amplification using QuikChange$^{XL}$ site-directed mutagenesis kit (Stratagene) and the mutagenized primer (5'GTTCAAGACCCCGACAAGGTAGAAGCC). Underlined characters indicate base substitutions.

### Cell transfection and immunohistochemistry

HeLa cells and 661W cells (11) were grown at 37°C and 5% $CO_2$ in DMEM supplemented with 10% FBS, penicillin (100U/ml) and streptomycin (50μg/ml).

HeLa cells were seeded on covereslips while 661W cells were seeded on ECM substrate (Sigma, Milan, Italy) at the concentration of $10^4$ per $cm^2$. Cells were cultured overnight and transfected with 0.4μg of DNA using PolyFect transfection reagent (Qiagen, Milan, Italy) according to the manufacturer's instructions. 661W cells were cultured for one day after transfection and then treated with 4mM Na Butyrate, 50μM taurine and 50ng/ml EGF.

For either transcription or translation or proteasome inhibition 24 hours after transfection HeLa cells were treated for 6 hours with either actinomycin D (5μg/ml, SIGMA, Milan, Italy) or α-amanitin (50μg/ml, SIGMA, Milan, Italy) or the proteasome inhibitor carbobenzoxy-L-leucyl-L-leucyl-L-leucinal (MG132, 50μM in DMSO, Calbiochem, Darmstadt, Germany) or cycloheximide (0.1μg/μl, SIGMA, Milan, Italy).

As primary antibodies we used: anti-human PRPF3 (clone 4E3, MBL, Japan) 1:200, anti-His tag (Qiagen, Milan, Italy) 1:50, anti-SC35 (SIGMA, Milan, Italy) 1:200, anti-Sm proteins (clone Y12, Lab Vision Corporation, Milan, Italy) 1:100, anti- Fibrillarin (72B9) 1:10 (23), anti-coilin (clone pd, SIGMA, Milan, Italy) 1:100, anti-Rhodopsin (RET-P1, SIGMA, Milan, Italy) 1:10000. Slides were photographed using a Zeiss Axioplan microscope.

Immunohistochemistry was performed on cryosections of human retinas (a donation of the Italian Eye Bank, "Fondazione Banca degli Occhi del Veneto" Venice; two different individuals were analyzed). Retinas were incubated with anti-human PRPF3 and stained using Vectastain ABC kit (Vector laboratories, Burlingame, CA, USA) following manufacturer's instructions. Images were acquired by the AxioCam MRc camera (Carl Zeiss), using the Axiovision 3.0 software (Carl Zeiss), with a format of 1030 x 1300 pixel.

**In situ hybridization**

The *Prpf3* antisense probe was obtained by linearization of the EST clone 5344086 (IMAGE) with *EcoRI* and transcription with T7 RNA polymerase. Digestion of the same plasmid with

*XhoI* and transcription with SP6 RNA polymerase generated the sense control probe. Eyes at postnatal day 8 (P8) and 2 month (Adult) old C57BL6 mice were analyzed by *in situ* hybridization on sectioned tissue as previously described (24).

**Retina electroporation**

All procedures on mice were performed in accordance with institutional guidelines for animal research. Wild type and T494M PRPF3-EGFP (PRP3-EGFP-pTriEx-1) were electroporated in neonatal CD1 mice. Newborn mouse pups were anesthetized by chilling on ice and eyelids were opened using a scalpel. After piercing the sclera with a 30-gauge needle, the DNA solution (6μg/μl) was delivered subretinally by using a Hamilton syringe as described (25). After DNA injection five 100V square pulses of 50ms duration were applied with a T820 electroporation system (BTX, San Diego, USA). Electroporated retinas were harvested 13 days after electroporation, fixed with 4% paraformaldehyde in PBS over night at 4°C. After cryoprotection with 30% sucrose in PBS and embedding in gelatin, cryosections (12μm) were cut on a cryostat. Retina sections were analyzed with Zeiss Axioplan microscope.

**ACKNOWLEDGEMENTS**

The authors would like to thank Dr. M. R. Al-Ubaidi, for providing 661W cells, the Fondazione Banca degli Occhi del Veneto for human tissue, Prof. P. Bouvet and Dr. M. Karali for reagents, Dr G. Meroni for valuable discussion concerning data. This work was supported in part by research grant from Fondazione Telethon to V.M., by research grants RETNET: MRTN-CT-2003-504003 and EVIGENORET: LSHG-CT-2005-512036 from the European Community to V.M. and S.S.B. Funding support is gratefully acknowledged by S.S.B from the Foundation Fighting Blindness (USA) and the Special Trustees of Moorfields Eye Hospital, London.

## CONFLICTS OF INTEREST

The authors declare that they have no conflicts of interest.

## REFERENCES


1. Vithana, E.N., Abu-Safieh, L., Allen, M.J., Carey, A., Papaioannou, M.G., Chakarova, C.F., Al-Maghtheh, M., Ebenezer, N.D., Willis, C., Moore, A.T. *et al.* (2001) A human homolog of yeast pre-mRNA splicing gene, PRP31, underlies autosomal dominant retinitis pigmentosa on chromosome 19q13.4 (RP11). *Mol. Cell,* **8,** 375-381.
2. McKie, A.B., McHale, J.C., Keen, T.J., Tarttelin, E.E., Goliath, R., van Lith-Verhoeven, J.J., Greenberg, J., Ramesar, R.S., Hoyng, C.B., Cremers, F.P. *et al.* (2001) Mutations in the pre-mRNA splicing factor gene PRPC8 in autosomal dominant retinitis pigmentosa (RP13). *Hum. Mol. Genet.,* **10,** 1555-1562.
3. Maita, H., Kitaura, H., Keen, T.J., Inglehearn, C.F., Ariga, H. and Iguchi-Ariga, S.M. (2004) PAP-1, the mutated gene underlying the RP9 form of dominant retinitis pigmentosa, is a splicing factor. *Exp. Cell Res,* **300,** 283-296.
4. Chakarova, C.F., Hims, M.M., Bolz, H., Abu-Safieh, L., Patel, R.J., Papaioannou, M.G., Inglehearn, C.F., Keen, T.J., Willis, C., Moore, A.T. *et al.* (2002) Mutations in HPRP3, a third member of pre-mRNA splicing factor genes, implicated in autosomal dominant retinitis pigmentosa. *Hum. Mol. Genet.,* **11,** 87-92.
5. Xu, S.Y., Schwartz, M., Rosenberg, T. and Gal, A. (1996) A ninth locus (RP18) for autosomal dominant retinitis pigmentosa maps in the pericentromeric region of chromosome 1. *Hum. Mol. Genet.,* **5,** 1193-1197.
6. Martinez-Gimeno, M., Gamundi, M.J., Hernan, I., Maseras, M., Milla, E., Ayuso, C., Garcia-Sandoval, B., Beneyto, M., Vilela, C., Baiget, M. *et al.* (2003) Mutations in

the pre-mRNA splicing-factor genes PRPF3, PRPF8, and PRPF31 in Spanish families with autosomal dominant retinitis pigmentosa. *Invest. Ophthalmol. Vis. Sci.,* **44,** 2171-2177.

7. Makarova, O.V., Makarov, E.M., Liu, S., Vornlocher, H.P. and Luhrmann, R. (2002) Protein 61K, encoded by a gene (PRPF31) linked to autosomal dominant retinitis pigmentosa, is required for U4/U6*U5 tri-snRNP formation and pre-mRNA splicing. *EMBO J.,* **21,** 1148-1157.
8. Kuhn, A.N., Reichl, E.M. and Brow, D.A. (2002) Distinct domains of splicing factor Prp8 mediate different aspects of spliceosome activation. *Proc. Natl. Acad. Sci. USA,* **99,** 9145-9149.
9. Gonzalez-Santos, J.M., Wang, A., Jones, J., Ushida, C., Liu, J. and Hu, J. (2002) Central region of the human splicing factor Hprp3p interacts with Hprp4p. *J. Biol. Chem.,* **277,** 23764-23772.
10. Maita, H., Kitaura, H., Ariga, H. and Iguchi-Ariga, S.M. (2005) Association of PAP-1 and Prp3p, the products of causative genes of dominant retinitis pigmentosa, in the tri-snRNP complex. *Exp. Cell Res.,* **302,** 61-68.
11. Tan, E., Ding, X.Q., Saadi, A., Agarwal, N., Naash, M.I. and Al-Ubaidi, M.R. (2004) Expression of cone-photoreceptor-specific antigens in a cell line derived from retinal tumors in transgenic mice. *Invest. Ophthalmol. Vis. Sci.,* **45,** 764-768.
12. Virtanen, I., Kivela, T., Bugnoli, M., Mencarelli, C., Pallini, V., Albert, D.M. and Tarkkanen, A. (1988) Expression of intermediate filaments and synaptophysin show neuronal properties and lack of glial characteristics in Y79 retinoblastoma cells. *Lab. Invest.,* **59,** 649-656.

13. Chen, T.J., Kuo, C.B., Tsai, K.F., Liu, J.W., Chen, D.Y. and Walker, A.M. (1998) Development of recombinant human prolactin receptor antagonists by molecular mimicry of the phosphorylated hormone. *Endocrinology,* **139,** 609-616.

14. O'Keefe, R.T., Mayeda, A., Sadowski, C.L., Krainer, A.R. and Spector, D.L. (1994) Disruption of pre-mRNA splicing in vivo results in reorganization of splicing factors. *J. Cell Biol.,* **124,** 249-260.

15. Keen, T.J., Hims, M.M., McKie, A.B., Moore, A.T., Doran, R.M., Mackey, D.A., Mansfield, D.C., Mueller, R.F., Bhattacharya, S.S., Bird, A.C. *et al.* (2002) Mutations in a protein target of the Pim-1 kinase associated with the RP9 form of autosomal dominant retinitis pigmentosa. *Eur. J. Hum. Genet.,* **10,** 245-249.

16. Anthony, J.G., Weidenhammer, E.M. and Woolford, J.L., Jr. (1997) The yeast Prp3 protein is a U4/U6 snRNP protein necessary for integrity of the U4/U6 snRNP and the U4/U6.U5 tri-snRNP. *Rna,* **3,** 1143-1152.

17. Lauber, J., Plessel, G., Prehn, S., Will, C.L., Fabrizio, P., Groning, K., Lane, W.S. and Luhrmann, R. (1997) The human U4/U6 snRNP contains 60 and 90kD proteins that are structurally homologous to the yeast splicing factors Prp4p and Prp3p. *Rna,* **3,** 926-941.

18. Santama, N., Dotti, C.G. and Lamond, A.I. (1996) Neuronal differentiation in the rat hippocampus involves a stage-specific reorganization of subnuclear structure both in vivo and in vitro. *Eur. J. Neurosci.,* **8,** 892-905.

19. Cairo, S., De Falco, F., Pizzo, M., Salomoni, P., Pandolfi, P.P. and Meroni, G. (2005) PML interacts with Myc, and Myc target gene expression is altered in PML-null fibroblasts. *Oncogene,* **24,** 2195-2203.

20. Sinclair, G.D. and Brasch, K. (1978) The reversible action of alpha-amanitin on nuclear structure and molecular composition. *Exp. Cell Res.,* **111,** 1-14.

21. Wehner, K.A., Ayala, L., Kim, Y., Young, P.J., Hosler, B.A., Lorson, C.L., Baserga, S.J. and Francis, J.W. (2002) Survival motor neuron protein in the nucleolus of mammalian neurons. *Brain Res.,* **945,** 160-173.

22. Schaffert, N., Hossbach, M., Heintzmann, R., Achsel, T. and Luhrmann, R. (2004) RNAi knockdown of hPrp31 leads to an accumulation of U4/U6 di-snRNPs in Cajal bodies. *Embo J.,* **23,** 3000-3009.

23. Roger, B., Moisand, A., Amalric, F. and Bouvet, P. (2002) Repression of RNA polymerase I transcription by nucleolin is independent of the RNA sequence that is transcribed. *J. Biol. Chem.,* **277,** 10209-10219.

24. Buniello, A., Montanaro, D., Volinia, S., Gasparini, P. and Marigo, V. (2004) An expression atlas of connexin genes in the mouse. *Genomics,* **83,** 812-820.

25. Matsuda, T. and Cepko, C.L. (2004) Electroporation and RNA interference in the rodent retina in vivo and in vitro. *Proc. Natl. Acad. Sci. U S A,* **101,** 16-22.

## LEGENDS TO FIGURES

**Figure 1. Expression and subcellular localization PRPF3.**

A: immunolocalization of the PRPF3 protein in adult human retina. onl: outer nuclear layer; inl: inner nuclear layer; gc: ganglion cell layer. Scale bar 100μm.

B, E, H and K: immunolocalization of PRPF3 in HeLa cells. C: immunolocalization of snRNPs with Y12 antibody. F: immunolocalization of SC35. I: immunolocalization of fibrillarin. L: immunolocalization of coilin. D, G, J and M show merged images and DAPI staining (blue) of nuclei.

HeLa cells were transfected with EGFP-tagged wild type (N), P493S mutant (O) and T494M mutant (P) PRPF3. Arrows indicate nucleolar localization of transfected PRPF3 protein. Scale bar in B - P: 10μm.

**Figure 2. Expression of transfected wild type and mutant PRPF3 in a photoreceptor cell line.**

Wild type and T494M mutant EGFP-PRPF3 were transfected in 661W cells and expression was analyzed with (B, D and E-Q) or without (A and C) treatment with sodium butyrate. Wild type PRPF3 localizes into the nucleus with a spotty patter (in green in panels A and B). T494M mutant PRPF3 aggregates inside the nucleus of 661W cells treated with sodium butyrate (green in panel D, arrow). T494D mutant PRPF3 maintains a spotty pattern inside the nucleus of 661W cells treated with sodium butyrate (green in panel E). Cells were also stained with an anti-rhodopsin antibody (red in A-E).

F-K: co-localization of EGFP-PRPF3 (green) and SC35 (red). Blue in merged images (H and K) is DAPI staining of nuclei.

L-Q: co-localization of EGFP-PRPF3 (green) and snRNPs (red). Blue in merged images (N and Q) is DAPI staining of nuclei.

**Figure 3. Expression of wild type and mutant PRPF3 in electroporated retina.**

Wild type and T494M mutant PRPF3 were *in vivo* electroporated in murine retinas. While wild type PRPF3 localizes inside the nuclei with a spotty pattern (blow-up in A), T494M mutant PRPF3 forms aggregates in photoreceptor nuclei (blow-up in B). Photoreceptors are defined based on histologial localization of nuclei in the retina section. Blue is DAPI staining of nuclei. Scale bar: 100μm.

**Figure 4. Expression of T494M mutant PRPF3 causes cell death in 661W photoreceptor cells**

A-H: 661W cells were transfected with either wild type (A-D) or T494M mutant EGFP-PRPF3 (E-H). After transfection cells were either treated (C-D and G-H) or not treated (A-B and E-F) with sodium butyrate. Nuclear localization of transfected proteins is shown in A, C, E, G. TUNEL staining is shown in B, D, F, H.

I: Time course of transfection experiments. Histogram reports percentage of transfected cells with either wild type PRPF3 (striped bars) or T494M mutant PRPF3 (black bars), percentage of trasfected cells presenting aggregate formation (gray bar) and undergoing apoptosis (white bar) after transfection with T494M mutant PRPF3.

**Figure 5. Effects of transcription, translation and proteasome inhibitors on wild type and mutant PRPF3 subcellular localization.**

HeLa cells were transfected with either wild type (A-C, G-I, M-O and S) or T494M (D-F, J-L, P-R and T-U) EGFP-PRPF3 (green) and immunolabelled with either anti-SC35 antibody (red in B, C, E, F, H, I, K, L, N, O, Q, R), or anti-snRNP antibody Y12 (red in S and T) or anti-fibrillarin (red in U). Cells were treated for 12 hours with either actinomycine D to block

transcription (A-F) or cycloheximide to block translation (G-L) or proteasome inhibitor (M-U). Merged images are shown in C, F, I, L, O, R-U where blue is DAPI staining of nuclei. T494M mutant PRPF3 aggregates inside the nucleolus (U). Scale bar: 10μm.

**Figure 1.**

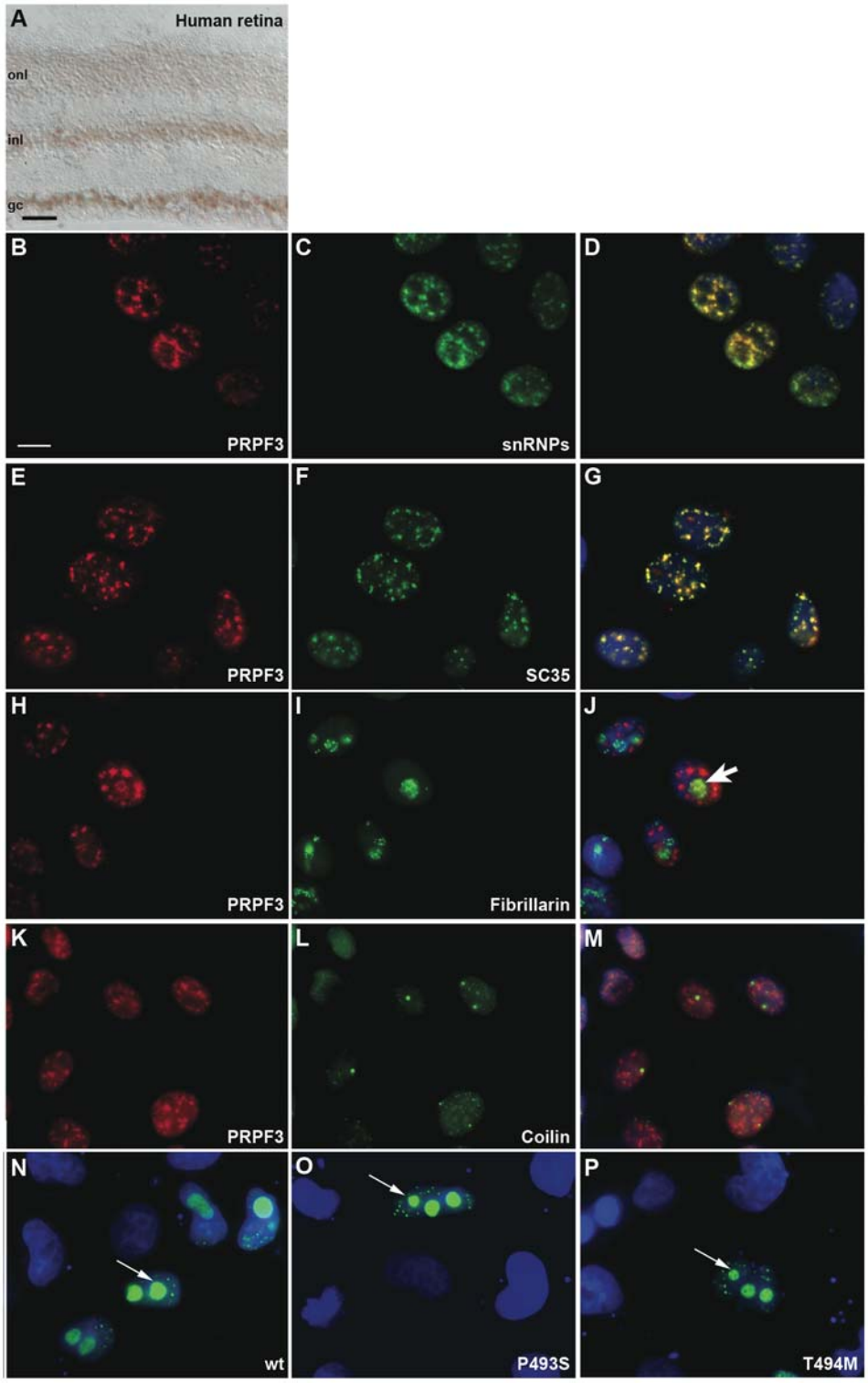
A
Human retina
onl
inl
gc
B
PRPF3
C
snRNPs
D
E
PRPF3
F
SC35
G
H
PRPF3
I
Fibrillarin
J
K
PRPF3
L
Coilin
M
N
wt
O
P493S
P
T494M

**Figure 2.**

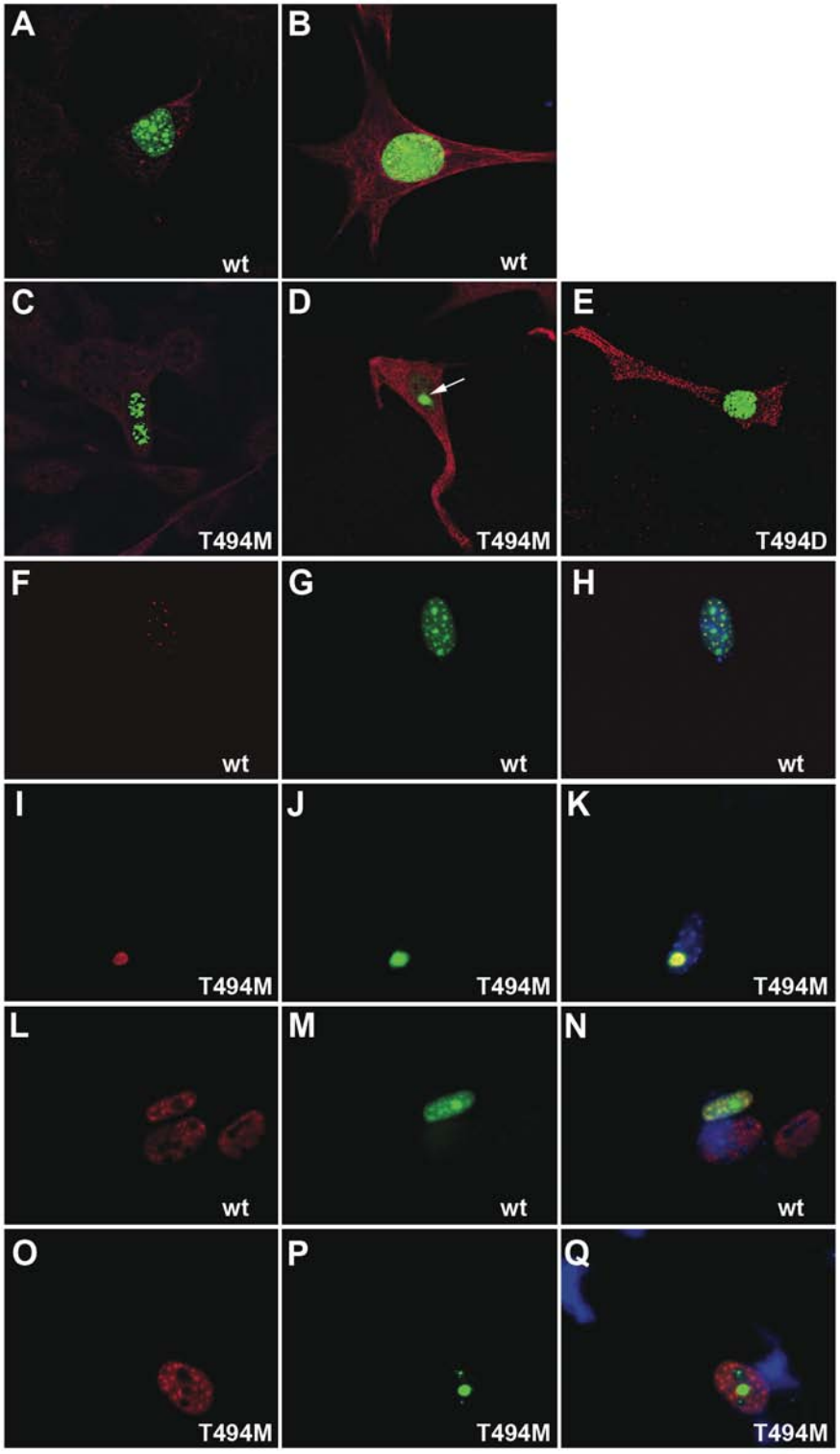
A
wt
B
wt
C
T494M
D
T494M
E
T494D
F
wt
G
wt
H
wt
I
T494M
J
T494M
K
T494M
L
wt
M
wt
N
wt
O
T494M
P
T494M
Q
T494M

**Figure 3.**

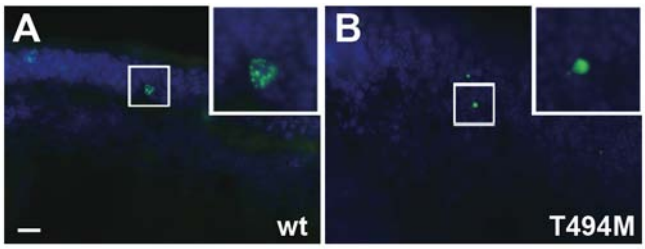

**Figure 4.**

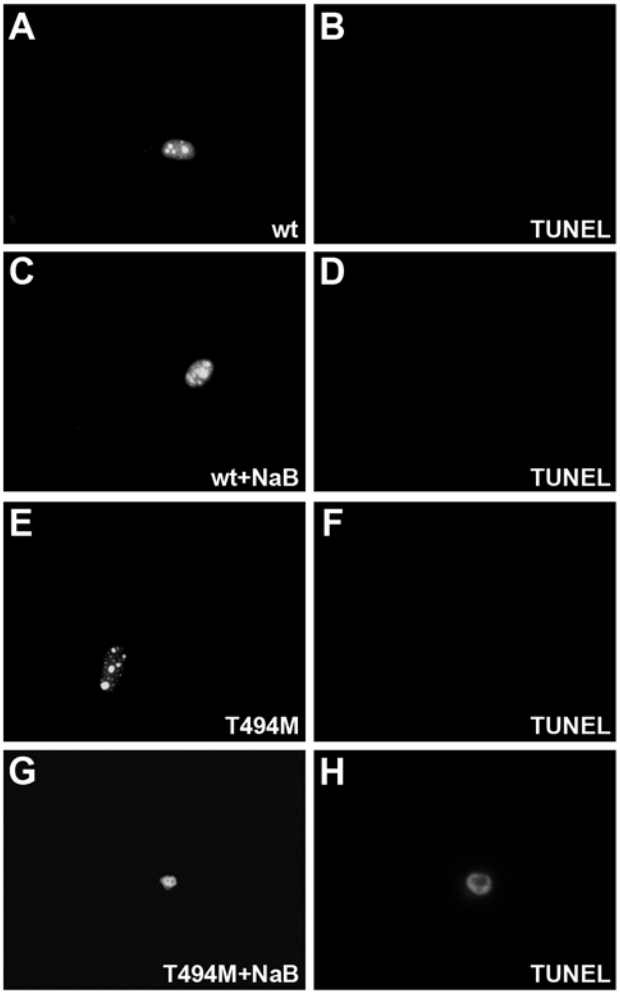
A
wt
B
TUNEL
C
wt+NaB
D
TUNEL
E
T494M
F
TUNEL
G
T494M+NaB
H
TUNEL

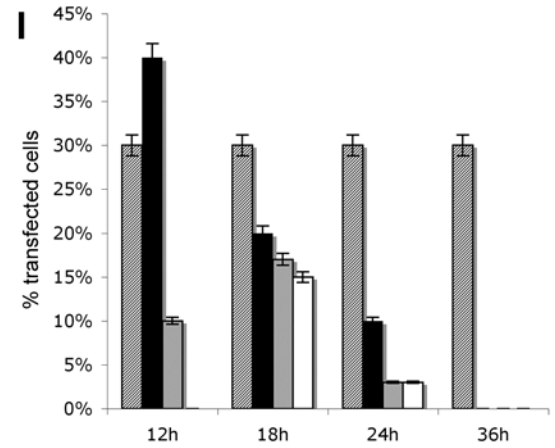
I
% transfected cells
45%
40%
35%
30%
25%
20%
15%
10%
5%
0%
12h
18h
24h
36h

**Figure 5.**

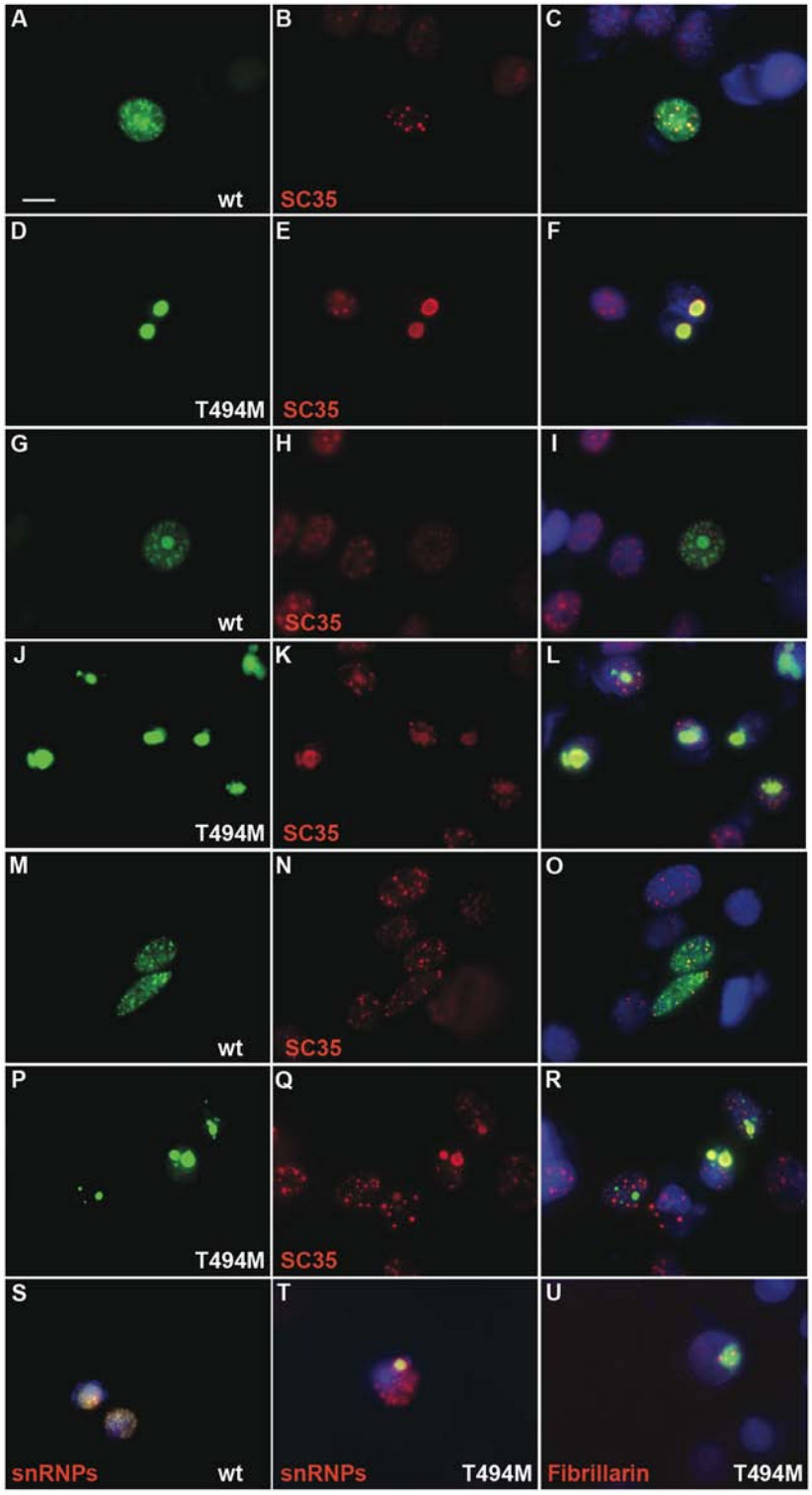
A
B
C
wt
SC35
D
E
F
T494M
SC35
G
H
I
wt
SC35
J
K
L
T494M
SC35
M
N
O
wt
SC35
P
Q
R
T494M
SC35
S
T
U
snRNPs
wt
snRNPs
T494M
Fibrillarin
T494M